

RAMAN LIGHT SCATTERING IN HYDROGENATED METAL-CARBON COMPOSITE FILMS

V. V. Uglov, A. K. Kuleshov,* M. P. Samtsov,
and M. V. Astashinskaya

UDC 535.375.54

We have used Raman scattering, elemental analysis, and structural analysis to study the effect of the concentration of incorporated metals (Cu, Ni) on the ratio of sp^2/sp^3 carbon bonds in composite hydrogen-containing films $a-C:H/Cu$ and $a-C:H/Ni$, formed by combining plasma-enhanced vapor phase deposition of carbon and sputtering of the metal, using a mixture of argon and methane or acetylene gases. We have shown that formation of a nanosized structure of metallic crystallites (2–5 nm) in the composite films leads to a significant increase in the fraction of disordered sp^3 -bonded carbon clusters and a decrease in the linear dimensions of the graphite-like carbon clusters.

Key words: Raman scattering, metal-carbon composite films.

Introduction. Raman spectroscopy has been successfully used as a nondestructive method for studying interatomic bonds in structurally different carbon materials such as diamond, graphite, diamond-like, amorphous, and polymer films [1, 2]. Study of composite metal-carbon films ($a-C:H/Me$) formed by vacuum methods is of considerable interest because of the possibility of a broad variation in their physical properties depending on the ratio of the intermolecular bonds in the carbon clusters, the rate of the chemical reaction between the metal and the carbon, and also the dimensions of metallic nanocrystals in the composite [3, 4]. The use of plasma chemical vacuum synthesis methods makes it possible to form low-dimensional systems in which metallic (≤ 50 nm) or carbide grains are incorporated into an amorphous carbon matrix, representing even smaller clusters (≤ 2 nm) with different types of bonds within them [5]. As a result, such nanocomposites acquire new physical properties compared with microcrystalline one-phase or macrocrystalline composite materials with one-phase structural formations larger than 100 nm. Doping by metals [6] is accompanied by a decrease in the internal mechanical stresses characteristic of diamond-like carbon, and the adhesion and wear-resistance of the composite film increase. As shown by model calculations and the experimental data, the ratio of the hardness to the modulus of elasticity and the degree of volumetric elastic recovery for the material after release of the strain for nanocomposite materials can exceed the corresponding values for microcrystalline composites and also very hard materials such as cubic boron nitride [7, 8]. From the data in [9] it follows that when forming composite $a-C:H/Cu$ films obtained by magnetron sputtering of a metal-graphite target in an argon-hydrogen plasma, as the copper content in the film increases, the intensity of the "D peak" in the Raman spectra increases, suggesting an increase in the fraction of graphite-ordered (sp^2 type bond) carbon clusters in the composite film. Increasing the cobalt content destroys the graphite ordering in $a-C:H/Co$ films obtained by the same method [10]. Increasing the fraction of carbide-forming metal in $a-C:H/W$ coatings does not change the quantitative characteristics of the Raman spectra [6]. The reasons for the observed phenomena have not been determined, since the effect of the metal or metal carbide crystallite sizes on the ratio of carbon bonds in composites has not been studied.

The aim of this work was to carry out a Raman spectroscopy study of the effect of the degree of doping by metals (both those that do not react with carbon and those that form carbides (Ni)) on the ratio of the types of bonds

*To whom correspondence should be addressed.

TABLE 1 Elemental Composition, Size of Metallic and Carbide Inclusions in *a*-C:H/Cu and *a*-C:H/Ni Films Obtained Using Plasma-Enhanced Chemical Vacuum Deposition Using Ar+C₂H₂ and Ar+CH₄ Gas Mixtures

Relative metal concentration, at.%	Reactant gas	Size of metallic formations, nm
<i>a</i> -C:H/Cu		
0.3	C ₂ H ₂	2 ± 2
0.9	C ₂ H ₂	3 ± 2
22	CH ₄	2 ± 2
75	CH ₄	8 ± 2
<i>a</i> -C:H/Ni		
60	CH ₄	3 ± 2

in carbon clusters in composite hydrogen-containing films *a*-C:H/Cu and *a*-C:H/Ni as related to the size and structural state of the metallic component.

Experimental procedure. Hydrogen-containing coatings were formed over a broad concentration range by plasma-enhanced chemical vacuum deposition of carbon and simultaneous sputtering of metal, using a mixture of reactant gases Ar+CH₄ and Ar+C₂H₂. Composite hydrogen-containing films *a*-C:H/Cu,Ni were deposited on substrates of single-crystalline silicon with (110) orientation, in a plasma reactor based on a distributed microwave gas discharge. The reactor is described in detail in [11]. In such a reactor, for the mixture Ar+carbon-containing gas (CH₄ or C₂H₂), activation conditions for electron cyclotron resonance with frequency 2.45 GHz and power up to 200 W were ensured. A potential of 300 V applied to the metal target enabled it to be sputtered and deposited on the sample holder. A floating potential was applied to the latter, which stimulated simultaneous deposition of carbon radicals from the resonance region. The pressure in the vacuum chamber was 0.13 Pa.

We used Rutherford back scattering to analyze the relative metal content (Me/Me+C) in the *a*-C:H/Cu,Ni films obtained. The results are shown in Table 1. The relative hydrogen concentration H/C was determined based on energy dispersive analysis of elastically reflected atoms, and was 35 ± 10 at.% for all the films. The copper, nickel, and nickel carbide grain size in *a*-C:H/Cu,Ni coatings was calculated from x-ray diffraction data using the formula in [12]: $\beta(hkl) = \lambda / (L \cos \theta)$, where $\beta(hkl)$ is the integrated width of the diffraction peak with the indicated *hkl*; λ is the wavelength of the incident radiation; L is the crystallite size; θ is the Bragg angle. In the case of *a*-C:H/Ni films, the size of metallic or carbide formations was determined for the range of relative nickel concentrations 0–60 at.%. The minimum size (3 ± 2 nm) occurs for a concentration of 60%. We took the Raman spectra at lower relative nickel concentrations (14 and 29 at.%). At these concentrations, the x-ray amorphous state of the film made it impossible to determine the crystallite size, but of course it is no greater than 3 ± 2 nm. The film thickness, measured by profilometry, was within the range 500–750 nm.

The Raman spectra for all the types of composite films were recorded at room temperature using a Spex 1403 (USA) spectrometer equipped with an R 928 photoelectron multiplier, cooled down to a temperature of 243 K. Excitation was carried out using an argon laser at $\lambda = 488$ nm for low power of the radiation at the sample (0.30–0.35 W), which did not lead to structural changes in the films.

As we know [1, 2], the Raman spectra from natural diamond crystals have a characteristic narrow line at 1331 cm⁻¹. In the case of perfect single crystals of graphite, we also observe one narrow line at 1581 cm⁻¹. In the Raman spectra from amorphous carbon, there are two broad overlapping bands in the regions 1330–1380 cm⁻¹ and 1540–1580 cm⁻¹, the "D" and "G" bands (Fig. 1a) [13]. In the case of graphite with crystallite grain size 2–30 nm (i.e., crystalline graphite), we observe similar but narrower bands [14]. In [1, 2], the *D* and *G* bands relate respectively to vibrations of the carbon atom of symmetry E_{2g} and A_{1g} in the model of an ideal graphite-like hexagonal ring of carbon atoms (Fig. 1b, c). Raman scattering of light in the visible region of the spectrum in *a*-C:H films is determined mainly by sp^2 -bonded rather than sp^3 -bonded carbon clusters, for which the resonant excitation condition is met for electronic transitions between π and π^* states on the edges of the valence band and the conduction band of graphite (for maximum scattering cross section) [2].

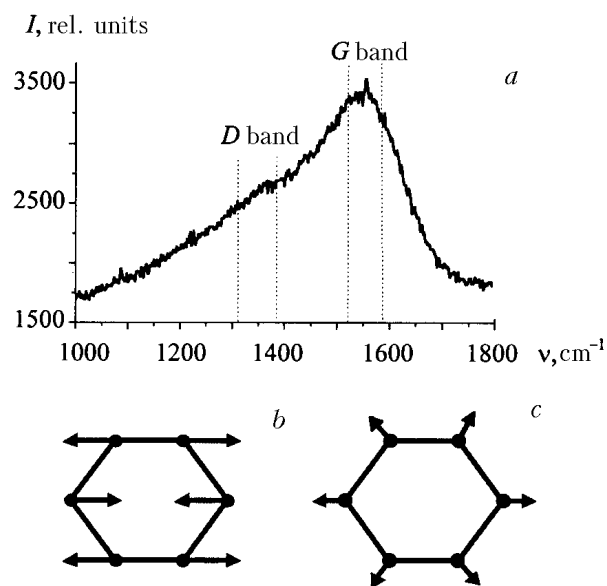


Fig. 1 Typical Raman spectrum from *a*-C:H film (a) and vibration of carbon atoms in an ideal planar graphite-like carbon ring. b) E_{2g} symmetry, c) A_{1g} symmetry.

We note that relative vibrations of the carbon atoms like the E_{2g} mode can also occur in other carbon structures, such as in carbon chains. Thus in [15] it is shown that in the Raman spectra, a band appears in the range 1500–1630 cm^{-1} (also including the *G* line) as a result of excitation of vibrations of both the aromatic carbon rings of the E_{2g} type and chain carbon fragments of various linear dimensions. Changes in the bond lengths and bond angles in the aromatic carbon ring lead to a shift in the maximum of the *G* band from the "ideal" position (1581 cm^{-1}) toward lower frequencies. The higher the degree of distortion in the carbon bonds, the greater the shift [16]. For strong conjugated C=C bonds, obviously vibrational frequencies greater than 1581 cm^{-1} are typical. As shown in [1], broadening of the *G* band $>50 \text{ cm}^{-1}$ and the shift in the maximum toward lower wavenumbers are connected with a decrease in the sizes of the carbon clusters ($<2 \text{ nm}$).

The broad *D* band with maximum in the 1340–1370 cm^{-1} region appears in disordered graphite films, and it is associated with modes of type A_{1g} for carbon clusters joined only into graphite-like aromatic rings [2]. The greater the linear dimension of the graphite-like cluster, i.e., the greater the number of planar hexagonal carbon rings joined into a cluster, the higher the intensity of the *D* band. Consequently, it is specifically the *D* band rather than the *G* band that can serve as an indicator for ordered aromatic clusters with sp^2 carbon bonds in an amorphous carbon structure.

In order to separate the *D* and *G* peaks in the experimental spectra, with computer modeling we used two gaussian functions and a linear background function. In order to estimate the linear dimensions (L_a) of the planar carbon clusters consisting of graphite-like rings, we used the ratio between the intensities of the *D* and *G* peaks $I(D)/I(G)$ and $L_a: I(D)/I(G) = C'(\lambda)/(L_a)^2$, where $C' = 0.0055$ is a constant determined for the wavelength of the exciting laser, 515.5 nm. The wavelength 515.5 nm is close to the exciting laser wavelength used in our work. The given ratio for estimating L_a is justified by the authors of [2] on going from crystalline graphite to amorphous graphite with $L_a < 2 \text{ nm}$. In this case, the ratio $I(D)/I(G)$ decreases from 2.2 to zero with a interrelated decrease in L_a from 2 to 0.142 nm, the maximum interatomic distance in a six-atom ring of carbon atoms.

Results and discussion. Fig. 2 shows the Raman spectra for *a*-C:H/Cu films obtained by combining plasma-enhanced chemical vacuum deposition of carbon and sputtering of the metal. In the Raman spectra, there are two overlapping bands (*G* and *D*) in the regions 1320–1390 cm^{-1} and 1560–1600 cm^{-1} . The results of mathematical separation of the *G* and *D* lines as gaussian curves are shown in Table 2. The Raman spectrum of the *a*-C:H film is characterized by the wavenumber for the *G* line, practically coinciding with the "ideal" value (1581 cm^{-1}) for vibrations of graphite-like aromatic rings. Consequently, graphite-like carbon clusters predominate in the structure of the film. How-

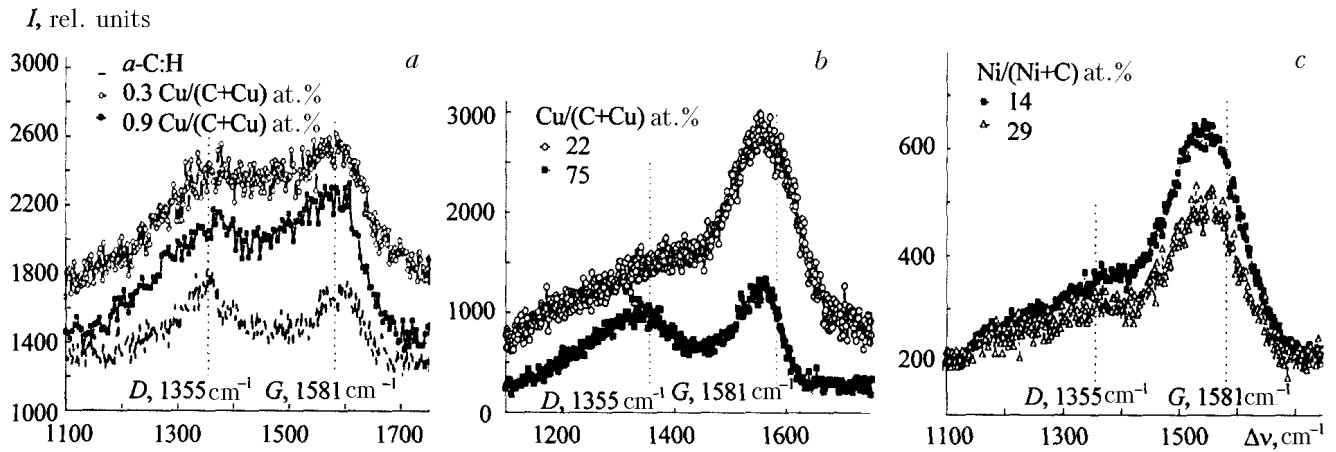


Fig. 2 Raman spectrum of hydrogen-containing *a*-C:H/Cu (a, b), *a*-C:H/Ni (c) films, formed using plasma-enhanced vacuum deposition using the reactant gas C₂H₂ (a, b) and the reactant gas CH₄ (c).

TABLE 2 Results of Mathematical Treatment of Raman Spectra From *a*-C:H/Cu and *a*-C:H/Ni Films Obtained Using Ar+C₂H₂ and Ar+CH₄ Gas Mixtures As a Function of the Relative Concentration of Cu and Ni in the Composites

Relative metal concentration, at.%	Reactant gas	<i>D</i> peak, cm ⁻¹	<i>G</i> peak, cm ⁻¹	Δ <i>D</i> , cm ⁻¹	Δ <i>G</i> , cm ⁻¹	<i>I</i> (<i>D</i>)/ <i>I</i> (<i>G</i>)	<i>L</i> _a , nm
<i>a</i> -C:H/Cu							
0	C ₂ H ₂	1356	1583	162	87	0.9	1.3
0.3	C ₂ H ₂	1380	1583	208	122	1.0	1.3
0.9	C ₂ H ₂	1376	1575	213	112	0.9	1.3
22	CH ₄	1350	1557	280	135	0.3	0.8
75	CH ₄	1335	1551	196	78	0.8	1.2
<i>a</i> -C:H/Ni							
14	C ₂ H ₂	1393	1550	284	114	0.4	0.9
29	C ₂ H ₂	1387	1550	304	108	0.4	0.9

Note. Δ is the halfwidth at half maximum of the corresponding peak.

ever, the broadening of the *G* peak is greater than 50 cm⁻¹, and the ratio of the intensities *I*(*D*)/*I*(*G*) is much less than 2.2. According to the above discussion, such parameters of the spectrum suggest that this film does not have the structure of crystalline graphite and it is amorphous. For such a film, we can use the estimate described above for the linear dimensions of the carbon clusters, which gives the value 1.3 nm (Table 2). The estimate of the fraction of *sp*³-bonded carbon-hydrogen clusters in *a*-C:H films proposed in [2] is based on the interrelationship between the wavenumber of the maximum of the *G* peak and the intensity ratio *I*(*D*)/*I*(*G*), with number of *sp*³ carbon bonds exactly determined using such experimental methods as NMR and electron energy loss spectroscopy. Using this estimate and drawing on the data in [2] and the parameters we obtained for the *G* and *D* lines of *a*-C:H films allowed us to determine the fraction of *sp*³ carbon bonds: 20%.

Doping the *a*-C:H film with even a small fraction of copper, when the relative copper concentration is no greater than 1 at.% (see Table 2), leads to appreciable broadening of the *G* and *D* lines without a change in the position of their maxima and the intensity ratio *I*(*D*)/*I*(*G*). This suggests slight distortions of the carbon bonds in the

graphite-like planar carbon clusters, with no change in their maximum dimensions or the fraction of sp^3 -bonded clusters in the composite a -C:H/Cu film. When the relative atomic concentration of copper increases up to 22% in the case of films deposited by the same method but using the gas mixture Ar+CH₄, greater changes occur in the Raman spectra. The degree of broadening of the G and D lines increases even more, the intensity ratio $I(D)/I(G)$ decreases down to 0.3, the position of the G peak goes below 1581 cm⁻¹ (which is typical for crystalline graphite) and is shifted toward lower frequencies compared to 1581 cm⁻¹. The size of the carbon clusters decreases by almost a factor of two (see Table 2). Thus fragmentation occurs along with disordering of the graphite-like planar carbon clusters, and an increase in the fraction of small carbon fragments and in the fraction of the sp^3 -bonded carbon-hydrogen clusters by up to 40%.

When nickel is incorporated into an a -C:H film with relative concentration in the range 14–29 at.% (see Table 2), we observe changes in the Raman spectra similar to those described above for a -C:H/Cu films with copper concentration 22 at.%. Consequently, incorporation of a carbide-forming metal in this concentration range, as in the case of copper which does not react with carbon, leads to significant disordering and fragmentation of not only graphite-like planar carbon clusters but also chain fragments. In this case, the fraction of sp^3 -bonded carbon-hydrogen clusters increases up to 40%. Note that for high copper content in an a -C:H/Cu film (75 at.%) obtained using active CH₄ gas, changes occur in the parameters of the G and D lines of the spectrum, suggesting partial ordering and an increase in the dimensions of the graphite-like planar clusters (see Table 2), but the ordering does not reach the level typical of the a -C:H film without incorporated metal. From Table 1, we see that the average size of the metallic crystals increases from 2 nm to 8 nm. The significant increase in the sizes of the metallic crystals means a decrease in the density of the boundaries between metallic and carbon clusters. The boundaries between clusters have a disordered structure, and the decrease in the volume fraction of the boundaries determines the ordering of the structure of the carbon clusters.

Conclusion. As follows from our analysis, an increase in the relative concentration of the metals Cu, Ni in the range 0–29 at.% in the carbon matrix of a -C:H/Cu,Ni films, obtained using plasma-enhanced chemical vacuum deposition, is accompanied by a decrease in the sizes of the graphite-like carbon clusters, an increase in the degree of their disordering and accordingly an increase in the content of sp^3 -bonded carbon clusters. The maximum distortions of the carbon-hydrogen matrix for composite a -C:H/Cu,Ni films occur as a result of the decrease in the size of the metal or metal carbide crystallites down to sizes (2–3 nm) comparable with the sizes of the carbon clusters (1–2 nm). For high copper concentration in an a -C:H/Cu film (75 at.%), the size of the metallic crystallites exceed the size of the carbon clusters several-fold, and consequently the volume of the disordered regions between the metal and carbon clusters decreases, which ensures the observed partial ordering of the carbon matrix in the composite film.

REFERENCES

1. J. Robertson, *Mater. Sci. Eng.*, **37**, 129–281 (2002).
2. C. Ferrari and J. Robertson, *Phys. Rev. B*, **61**, 14095–14106 (2000).
3. B. Feng, D. M. Cao, W. J. Meng, L. E. Rehn, P. M. Baldo, and G. L. Doll, *Thin Solid Films*, **389**, 210–216 (2001).
4. I. Gerhards, C. Ronning, U. Vetter, H. Hofsass, H. Gibhardt, G. Eckold, Q. Li, S. T. Lee, Y. L. Huang, and M. Seibt, *Surface and Coatings Technology*, **158–159**, 114–119 (2002).
5. Y. Pauleau, F. Thiery, P. B. Barna, F. Misjak, A. Kovacs, S. N. Dub, V. V. Uglov, and A. K. Kuleshov, *Rev. Adv. Mater. Sci.*, **6**, 140–149 (2004).
6. C. Strondl, N. M. Carvalho, J. Th. M. De Hosson, and G. J. Kolk, *Surface and Coatings Technology*, **162**, 288–293 (2003).
7. S. Veprek and A. S. Argon, *Surface and Coatings Technology*, **146–147**, 175–182 (2001).
8. J. Musil, *Surface and Coatings Technology*, **125**, 322–330 (2000).
9. E. A. Smorgonskii, T. K. Zvonareva, E. I. Ivanova, I. I. Novak, and V. I. Ivanov-Omskii, *Fiz. Tverd. Tela*, **45**, No. 9, 1579–1589 (2003).
10. Rusli, S. F. Yoon, Q. F. Huang, J. Ahn, Q. Zhang, H. Yang, Y. S. Wu, E. J. Teo, T. Osipowicz, and F. Watt, *Diamond and Related Mater.*, **10**, 132–138 (2001).

11. Y. Pauleau, F. Thiery, V. V. Uglov, A. K. Kuleshov, S. N. Dub, and M. P. Samtsov, *Rev. Adv. Mater. Sci.*, **4**, 1–8 (2003).
12. S. S. Gorelik, Yu. A. Skakov, and L. N. Rastorguev, *X-ray Diffraction and Electronic/Optical Analysis* [in Russian], Metallurgiya, Moscow (2002).
13. V. V. Uglov, A. K. Kuleshov, D. P. Rusalsky, M. P. Samzov, and A. N. Dementshenok, *Surface and Coating Technology*, **158–159**, 699–701 (2002).
14. M. C. Rossi, S. Salvatori, P. Ascarelli, E. Cappelli, and S. Orlando, *Diamond and Related Mater.*, **11**, 819–823 (2002).
15. D. Lin-Vien, N. E. Coltharp, W. G. Fateley, and J. G. Graselli, *The Handbook of Infrared and Raman Characteristic Frequencies of Organic Molecules*, Academic Press, New York (1991).
16. E. D. Obratsova, M. Fiyii, S. Hayashi, V. L. Kuznetsov, Yu. V. Butenko, and A. L. Chuvilin, *Carbon*, **35**, No. 5–6, 821–828 (1998).